공학석사 학위논문

Development of an optoelectronic neural stimulator using a photovoltaic cell integrated with a light emitting diode for in-vivo optogenetics

생체 광유전학 연구를 위한 발광다이오드와 광전지가 집적된 광전자 신경 자극기의 개발

2017년 2월

서울대학교 융합과학기술대학원

융합과학부 나노융합전공

최 나 라

Development of an optoelectronic neural stimulator using a photovoltaic cell integrated with a light emitting diode for in-vivo optogenetics

지도교수 송 윤 규

이 논문을 공학석사 학위논문으로 제출함

2017년 1월

서울대학교 융합과학기술대학원

융합과학부 나노융합전공

최 나 라

최나라의 석사 학위논문을 인준함

2017년 1월

위 원 장 박 원 철 (인)

부 위 원 장 송 윤 규 (인)

위 원 이 강 원 (인)

Abstract

Development of an optoelectronic neural stimulator using a photovoltaic cell integrated with a light emitting diode for in-vivo optogenetics

Na Ra Choi

Program in Nano Science and Technology

Department of Transdisciplinary Studies

The Graduate School of Convergence Science and Technology

Seoul National University

Neural stimulation by light in optogenetics present a new approach to stimulate targeted neuron compared to electrical stimulation that affects another cell. This paper indicates the development of a wireless implantable optoelectronic neural stimulator for optogenetic research using photovoltaic (PV) cells and light emitting diodes (LEDs). The micro LED was used to stimulate the photo-responsible cells and the PV was coupled together to turn on the LED. The GaAs-based PV device is designed near infrared light with high tissue penetration, and it is made of a tandem structure composed of three layers with optimized height to increase the absorption rate of light. Using the standard micro-electronic fabrication process, the PV and the LED were made and bonded. The stimulator was designed in the shape of a micro-

sized cube with 400 μm sides. It is small enough to be implanted in the brain and also possible for deep brain stimulation. In this experiment, we demonstrated that PV can generate enough energy to turn on the LED with high efficiency of 34 %. And we show that the emitted light of the stimulator can stimulate the HEK cell using patch clamp set-up. Therefore, the induced photocurrents by our stimulator would be sufficient enough to evoke neuronal firing if our stimulator was implanted in the mammalian brain.

Keywords : Optogenetic, Optoelectronic, Neural Stimulator, Photovoltaic cell, light emitting diode

Student Number : 2014-24885

Contents

List of Tables

List of Figures

Chapter 1. Introduction

1.1. Optogenetic

Neural stimulation by light in optogenetics is a method of stimulating neurons. In comparison to traditional electrical stimulation where localization of the stimulus to an individual neuron is difficult with the neurons in the neighborhood of the target neuron affected, the optogenetic approach allows individual neurons to be stimulated. Electrical stimulation is the most common technique applied in modern medicine and improved over the years. However, as it generally affects neighborhoods of neurons it makes the classification of a single cells mechanism difficult and hence the also the nerve system. One solution proposed to overcome the cell selectively of the electrical method is optical stimulation through optogenetics. Channelrhodopsin-2 (ChR2) proteins are a blue light photosensitive membrane protein and are well expressed in the membrane region as well as inside the neuron cell. The ChR2 channel is a light-activated cationic channel that opens the cannel and allows cations to enter and exit neural cell. Due to the cation entrance exit, current flows through the cell and the electrical signal is transmitted. After expressing the protein in the targeted cells, then light is emitted, only the cells expressing ChR2 excite. Since ChR2 excites in the blue light of the wavelength range of 450~480 nm, the use of blue light to stimulate ChR2-expressing cells is an optogenetic tool (Nagel et al.

2003; Boyden et al. 2005; Han et al. 2009; Deisseroth 2011; Diester et al. 2011; Packer et al. 2013; AzimiHashemi et al. 2014; Schneider et al. 2015).

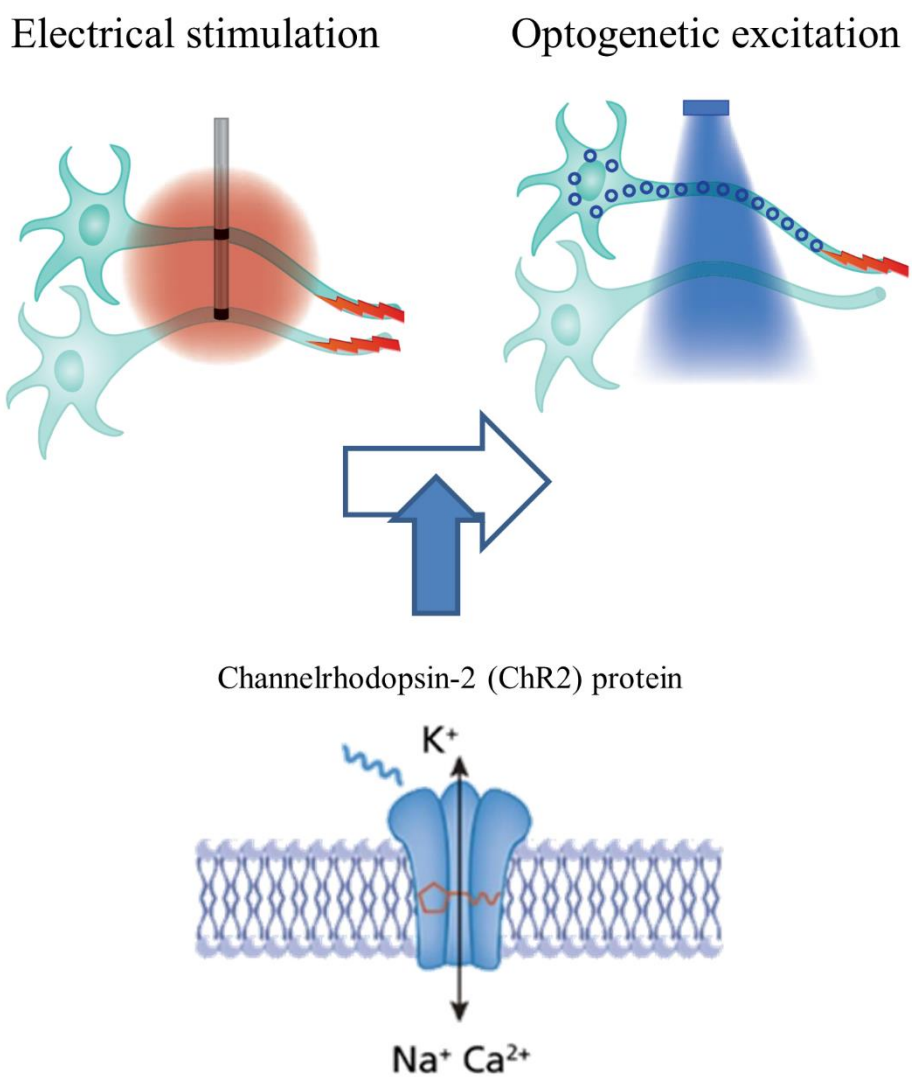

Figure 1. Targeted neural cell excitation in optogenetics with a blue light-activated channelrhodopsin-2 (ChR2) protein (Deisseroth 2011; Packer et al. 2013).

.

1.2. **Motivation**

A blue light has a short wavelength and hence low tissue penetration; therefore, the light must be induced close to the target cell. Previous studies of cell stimulation by optogenetics have addressed this problem and varieties of methods have been developed to deliver the blue light to the target cell (Huber et al. 2008; Anikeeva 2013; Warden et al. 2014; Lee et al. 2015; Pisanello et al. 2016). Many researchers including have investigated the delivery of light using a light waveguide (optical fiber): (Zhang et al. 2009; Wang et al. 2012; Lu et al. 2014; Son et al. 2014). The main drawback of this method is the spatial limit of the waveguide itself. Another method is to insert a microchip together with a blue light μ-Light Emitting Diode (LED) into the brain which is powered wirelessly as presented by (Kim et al. 2013; Kwon et al. 2014). In this case, the chip is not fully implantable and must be fixed to the skull, or the transceiver used to wirelessly receive power must be installed separately. Instead of delivering blue light directly to cell, a research team used a photovoltaic (PV) cell which absorbs the near infrared light (NIR) with high penetration depth in tissue (Abdo et al. 2011). The PV cell converts NIR from optical fiber to electrical energy for stimulating neural cells. However, it is electrical stimulation and stimulate non-selective target cell.

Considering previous researches, we have attempted to use NIR with deep

penetration depth as an energy source to compensate for the drawbacks of using blue light. When combined with NIR light and blue light, it is possible to transfer energy to deep brain and have specific cell selectivity that is an advantage of optogenetic method. We planned a device with both of these advantages and designed it to be micro-size and fully implantable to reduce tissue damage and spatial limitation when it implants in brain. The device will be developed to compensate for the shortcoming of previous studies and will show improved performance.

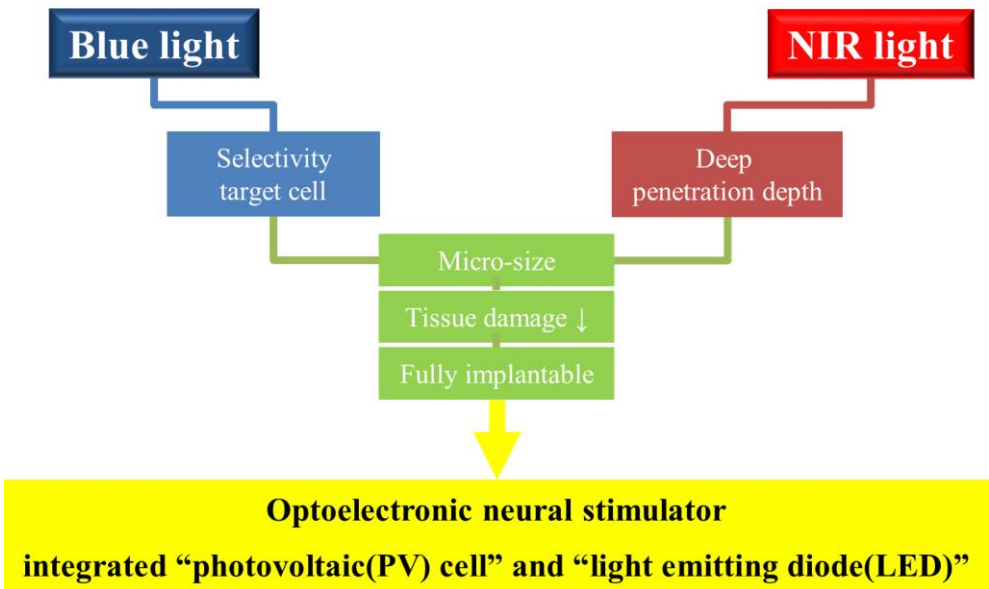

Figure 2. Diagram of motivation to develop optogenetic neural stimulator with a blue light and a near infrared light.

1.3. Blue light and near infrared (NIR) light

NIR light could cover much more of the brain than blue light. The penetration depth of the blue light of 450~480 nm wavelength, which can stimulate ChR2, is 0.4 mm. The NIR light has a penetration depth of 1.5 mm which is three times greater than that of blue light (Eggert and Balazek 1987). Compared to the actual cortical layer length of mammal brain, the blue light does not penetrate the cerebral cortex with a length of 1.21 mm in the mouse. In contrast, NIR light is able to penetrate entirely the cerebral cortex of the mouse. In the human cerebral cortex with 2.622 mm-depth, the IV layer with the largest neuron population and the V layer with the largest number of pyramidal cells controlling the motor nerves are also accessible in Figure 3 (Defelipe 2011). The cerebral cortex deals with important functions such as memory, attention, perception, awareness, thought, language, and consciousness. The primary motor cortex in the II-V layers is concerned with all voluntary movement that can move the skeletal muscle. The specific muscle on the opposite side of the body is contracted by stimulating the primary motor cortex, depending on the stimulation site. These muscle movements can be seen in the body part and the somatotopical arrangement is very clear. The giant pyramidal cell of Betz, the largest of the pyramidal cells located in the V layer, mainly controls the muscles of the legs.

Using the NIR light as an energy source, the device can stimulate pyramidal cells

located in II-IV layers of cerebral cortex, as well as the giant pyramidal cells of Betz located in V layer. This may help to map neurons and muscle network and may be useful in treatment studies of motor nerve damage and disease.

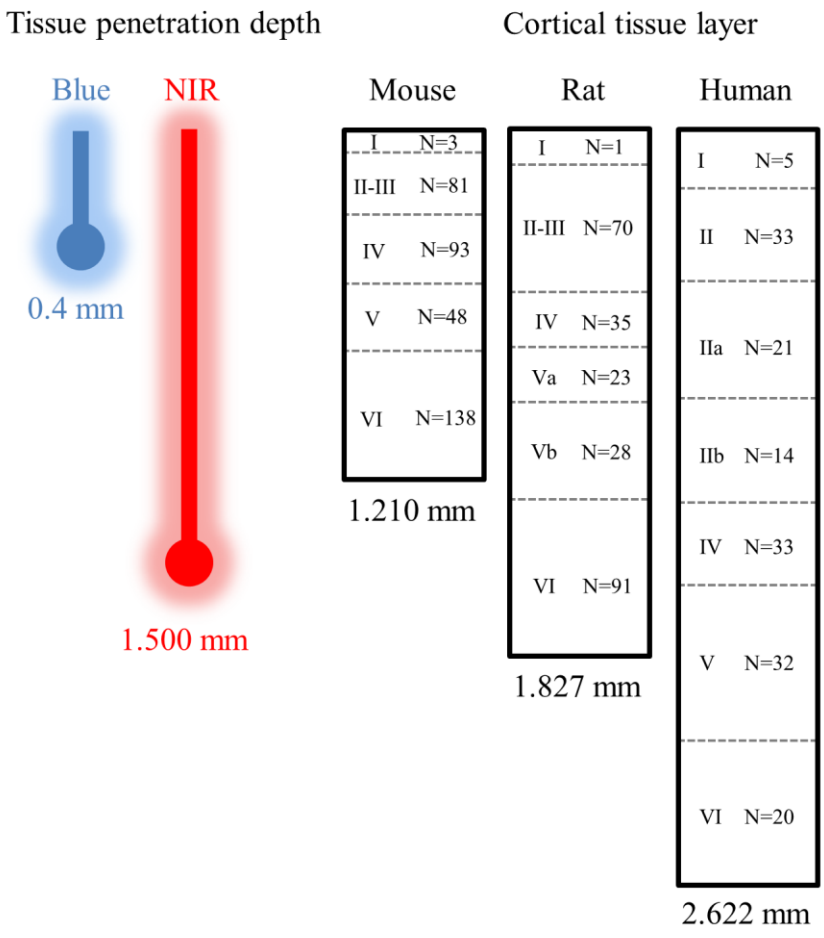

Figure 3. Brain tissue penetration depth comparison of blue light and near infrared light and cortical tissue layer variation between humans, rats and mice (Eggert and Balazek 1987; Defelipe 2011).

1.4. **Optoelectronic neural stimulator**

In this paper, a wireless stimulator consisting of an integrated LED and photovoltaic (PV) cell. The PV cell converts optical energy into electrical energy, and the LED converts the electric energy back into optical energy as blue light. The PV cell is designed to absorb near infrared light (NIR; 850~870 nm), which has high tissue penetration properties. A schematic design of the bonding process and light pathway from incident NIR light to emitting blue light is shown in Figure 4. The NIR photons entering are absorbed by the 3 PV cells and the absorbed light can be converted simultaneously into electrical energy. The energy can operate the LED, which emits short wavelength blue light. Finally, the blue light from the LED stimulates the ChR2-expressing cell. The cell is a tandem structure providing high absorption efficiency. The LED is designed to emit blue light (450 nm) for stimulation of the ChR2-expressing neural cells. The stimulator constitutes the integration of the PV and LED into a single implantable device. The PV and the LED are formed as a concavo-convex structure for bonding after fabrication. After the process of fabrication and bonding, the final stimulator is 400×400×400 μm^3. The LED is bonded to the PV with silver epoxy in small bumps to prevent the epoxy from spreading laterally. The bonded device is covered with a UV-cured epoxy for encapsulation. The micro-size device is implantable and due to its small size limits tissue damage. The ability of the light produced by the device to stimulate ChR2 in

HEK293 cells has been confirmed and shows that the device can and can be utilized for long distance stimulation.

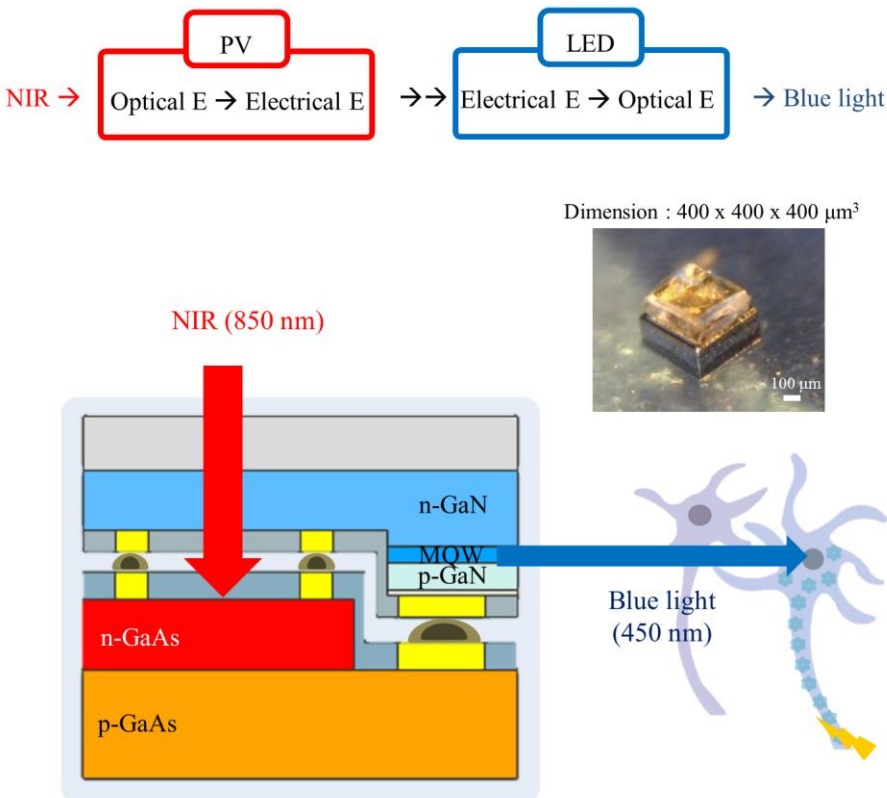

Figure 4. Schematic design of light pathway through the optoelectronic neural stimulator with dimension of 400 x 400 x 400 μm^3. Incident NIR light is transmitted through the stimulator and converted to blue light stimulating ChR2-expressing cells.

Chapter 2. Material and Method

2.1. Light emitting diode (LED) and photovoltaic (PV) cell

2.1.1. Light emitting diode (LED)

Light-emitting diode (LED) is a type of p-n junction diode, a semiconductor device that uses electroluminescence effect, which is a phenomenon in monochromatic light is emitted when forward bias is applied. When the forward voltage is applied, electrons in the n-layer and the holes in the p-layer are coupled to emit energy as much as the energy gap between the conduction band and the valance band. This energy is mainly emitted in the form of heat of light, the LED emits energy in the form of light. Gallium nitride (GaN) has a band gap energy of 3.4 eV at room temperature, it emits near ultraviolet light with 365 nm wavelength. Indium gallium nitride (InGaN) is a mix of GaN and InN. InGaN can emit blue light with a wavelength of 450 nm by adjusting Indium properly. In order to increase the coupling efficiency between electrons and holes, quantum well in which an active layer and barrier are alternately laminated is used. Multi quantum well (MQW) is a multi-layer structure of the quantum well. The MQW is composed of semiconductors with a smaller band gap between the larger band gap semiconductor, by lowering the quantum mechanical energy lever of the electron, it restrains electrons in the well and activates recombination of electrons and holes to emit light. For the high

luminescence efficiency, the highest quality crystal characteristics are required and the grow process is the most delicate for a long time. The light emitting layer is made of InGaN/GaN. In this paper, a GaN-based LED on sapphire substrate is used and consists of p-type GaN, 3 layers of MQWs, and n-type GaN. The LED was fabricated using the matalorganic chemical vapor deposition (MOCVD) method. The MOCVD is a method of depositing several thin layers continuously. A cross section layering of the GaN-based LED is shown in Figure 5 (a). Epitaxial layers including the InGaN multiple-quantum-well (MQW) were grown on sapphire wafers. The substrates were purchased from EpiVally co., Ltd.

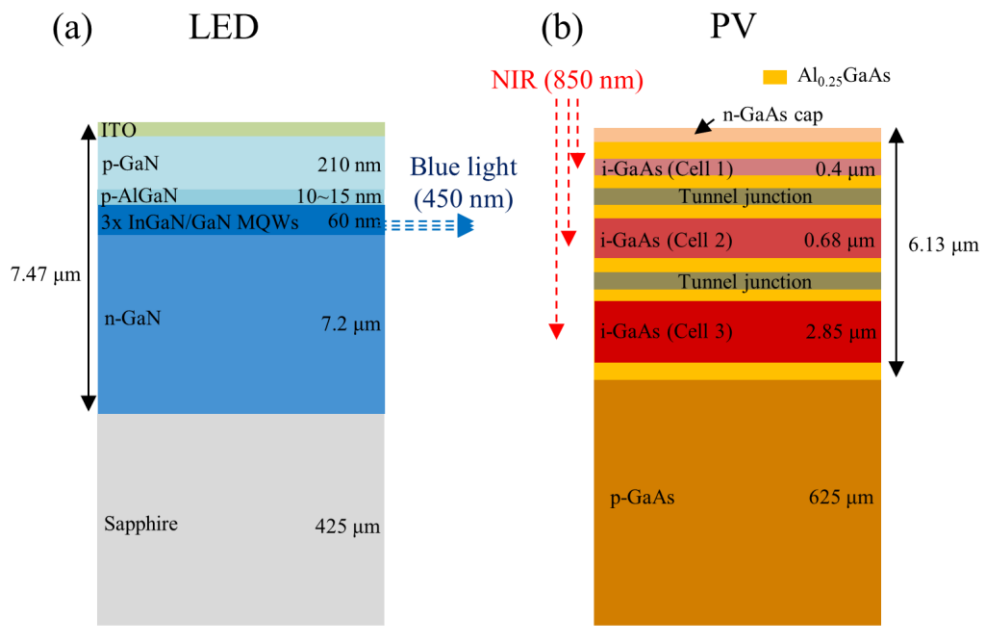

Figure 5. Cross-sectional layering schematic for (a) the LED and (b) the PV cell.

2.1.2. Photovoltaic (PV) cell

Photovoltaic (PV) cell is a semiconductor device that converts light energy into electrical energy. The light projected to the PV, electrons and holes are generated by photons. The electrons and holes diffuse to the periphery, the potential difference is formed, and these are separated by a strong electric field. The electrons diffused from the p-type semiconductor are directed toward the n-type semiconductor. The holes in the n-type semiconductor migrate to the p-type semiconductor, and current flows

PV was a single junction type until the mid-1990s. After the mid-1990s, dual junction cells appeared and triple junction was developed to increase efficiency in 1999. A multi junction PV cell is composed of several pn junctions and current flows through the tunnel junction. GaAs-based PV cell has a high light absorption coefficiency, it is possible to manufacture high efficiency PV cell with a thin film and is widely used in aerospace technology and research. GaAs is a compound semiconductor mixed gallium (Ga) and arsenic (As). Gallium is a by-product of the smelting aluminum and zinc. Arsenic is not rare but poisonous. GaAs is especially useful in multi-junction and high-efficiency PV cell for several reason. The GaAs has 1.43 eV band gap, nearly ideal for optimizing the single junction PV cell efficiency an absorptivity so high it requires a cell only a few micros-thick. Unlike

silicon cell, GaAs cells are relatively insensitive to heat. Its alloys as PV cell material is the wide range of design possible. A cell based GaAs can have several layers of slightly different composition to precisely control the generation and collection of holes and electrons.

Figure 5 (b) shows the PV cell consisting of a PN-junction of gallium-arsenide/aluminum-gallium-arsenide (GaAs/AlGaAs) heterostructure (Yamaguchi 1999; Song et al. 2007). A tandem structure was introduced to improve the absorption efficiency. The tandem structure consists of 3 p-i-n photovoltaic cells, each with an optimally designed intrinsic layer thickness and connected in series by two thin tunnel junctions. The top layer absorbs one-third of the incident photons, the middle cell absorbs half of the transmitted light and the last layer absorbs the rest.

2.2. **Concavo-convex structure design**

To bond the LED and the PV by p-p junction, p-type GaAs layer was exposed by removing 3 p-i-n photovoltaic cells with a thickness of 6.13 μm which is the top layer of the PV cell. The LED were also exposed to n-GaN by removing p-GaN and MQW layers. In this process, the absorption layer (3 p-i-n photovoltaic cells) of the PV and activation layer (MQW layer) of the LED are removed. On account of that, various concavo-convex designs are proposed to efficiently absorb and emit light. Since the active layer of the LED with a small area can emit enough light to stimulate cells, the light absorbing area of the PV is mainly compared. Design 3 has adopted the highest absorption of the PV compared to the LED emitting area among various designs. The LED has lateral dimensions of 400×400 μm^2. The p-metal pad of the LED is 70×70 μm^2, which is the light emitting region. The p-type GaAs of the exposed PV is 95×95 μm^2, bigger than the light emitting region of the LED. The PV window for entering NIR light has an area of 30000 μm^2.

Table 1. Comparison of optimal design of light window and light emitting portion.

	Design 1	Design 2	Design 3	Design 4	Design 5
	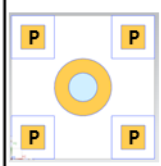	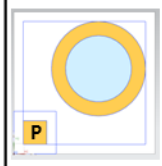		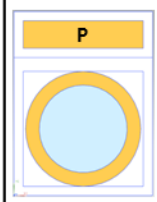	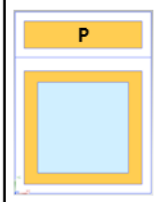
Single cell [μm^2]	400 x 400	400 x 400	400 x 400	400 x 500	400 x 500
PV [μm^2]	2827	15393	30000	22698	40000
LED [μm^2]	10000	2500	2500	15600	15600
PV/LED [%]	0.28	6.16	12	1.46	2.56

2.3. **Fabrication process**

The LED consists of an Indium-Tin-Oxide (ITO) (200 nm), p-type GaN (210 nm), MQW (60 nm) and n-type GaN (7.5 μm) on a sapphire substrate (420 μm). The PV cell consists of N-GaAs (6.13 μm) and p-type GaAs (625 μm). To bond the LED and the PV by p-p junction, the N-GaAs of the PV is removed to expose a 95×95 μm^2 of the p-type GaAs region and the LED is etched 6.13 μm deep leaving a 70×70 μm^2 emitting light region. Figure 6 shows the fabrication process of the LED and the PV. The LED process is shown in Figure 6 (a). 3 μm-thick photoresist (PR) is patterned using photolithography for a deep etch process. Dry etching was performed using gas mixed with Cl_3 (30 sccm) and BCl_3 (5 sccm) at 800 W power (Multiplex ICP, STS). The etching rate is 300 nm/min. After deposition of a 100 nm-thick SiN passivation layer by Plasma enhanced chemical vapor deposition (PECVD; UNaxis), the passivation layer was patterned for n- and p- contact pads and etched with BOE 30: 1. The etch rate of SiN using BOE 30:1 is 20 nm/min. Titanium (Ti) / Aluminium (Al) / Ti / Gold (Au) (1 / 100 / 30 / 100 nm) for p- contact metal and Ti / Al / Nickel (Ni) / Au (30 / 100 / 30 / 100 nm) for n- contact metal were deposited by electron beam evaporation (ULTECH). The Fabrication process of the PV cell is shown in Figure 6 (b). The same thick PR used in manufacturing the LED was patterned and etched. The N-GaAs layer was removed by wet etching. The PV was placed in a H_3PO_4 : H_2O_2 : H_2O (1:1:10) solution for 15 min (Cho et al. 1999). The etch rate of

N-GaAs is 420~480 nm/min. The exposed surface was protected through a 150 nm-thick SiO_2, followed by n- and p- contact pad patterning. The etch rate SiO_2 by BOE 30:1 was 100 nm/min. 10 nm of Ti and 100 nm of Au were deposited for the p-contact and 20 nm of Germanium (Ge), 50 nm of Ni, and 100 nm of Au were deposited for the n- contact (Shiraishi and Taeda 1998). For good Ohmic contact, the PV was annealed for 30 s at 400°C using the Rapid thermal annealing (RTA; RTA150H-SVP1, NYM TECH) method (Bruce and Piercy 1986; Lu et al. 1989)

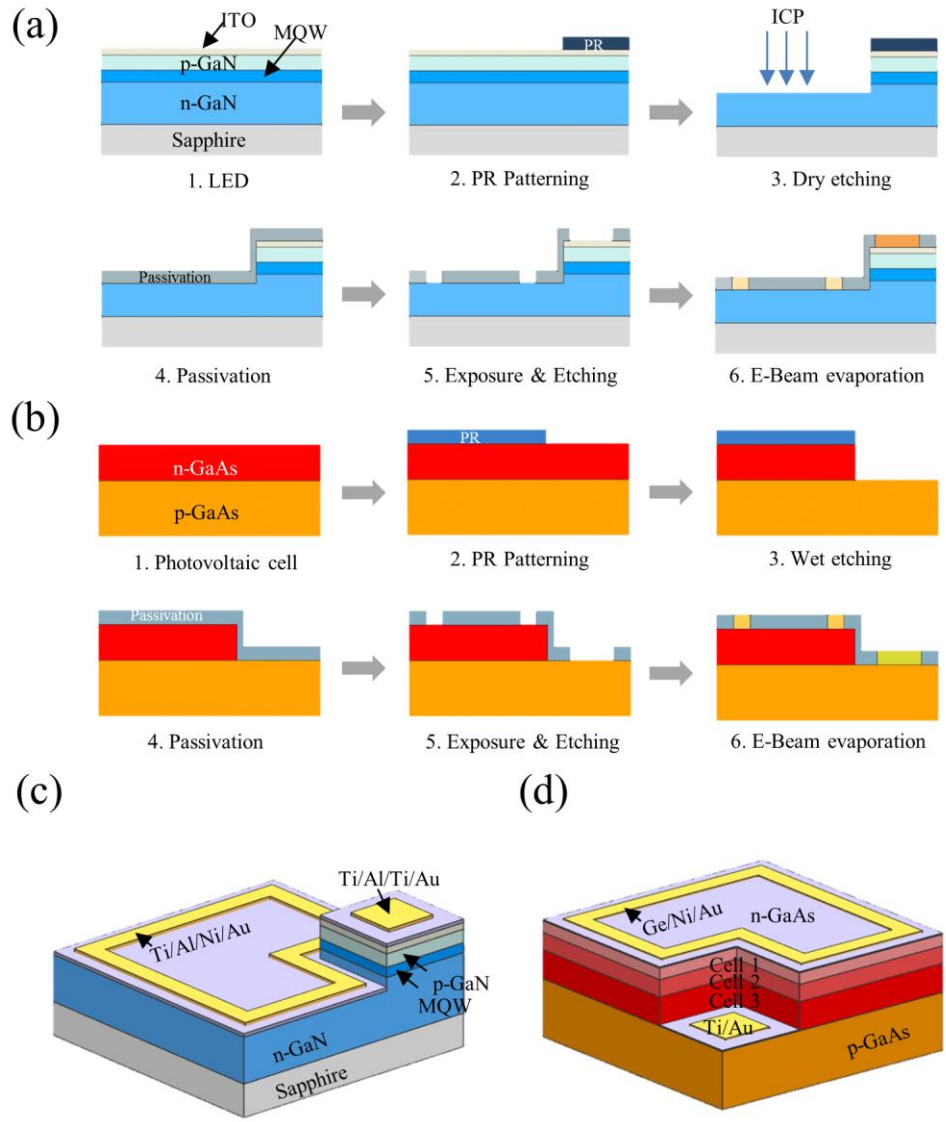

Figure 6. Schematic illustration of the fabrication process of the PV cell and the LED for concavo-convex bonding. (a) The LED was deep-etched 6 μm by dry etching and passivated with SiN (100 nm). The p-metal of the LED is composed of Ti/Al/Ti/Au (1/100/30/100 nm)

2.4. **Integration PV and LED**

The LED has a 420 μm-thick sapphire substrate and the PV has a 625 μm-thick P-type GaAs substrate. The sapphire substrate is lapped using a lapping machine (GMI) with a diamond suspension and a grooved alumina plate. The high hardness of sapphire makes the lapping process difficult to perform and control for the desired 200 μm thickness of the LED. The Lapping process was conducted on the LED 4~5 times for about 3~4 hours each time changing the rotation direction of the lapping machine and replacing the suspension. The thickness was also measured every 3~4 hours to control the final thickness. The lapping for the p-type GaAs of the PV was performed using a 5 micron alumina suspension (Buehler) and quartz plate. The PV sample was fixed to the lapping tool with wax. The butterfly motion was repeated during the 20 min process for fitness control. The suspension was replaced every 5 min due to the abrasiveness of the particles. The thickness of the PV cell was also measured every 5 min. For both the LED and the PV cell the final thickness was 200 μm. For isolation of the individual elements with 400×400 μm^2 area, dicing was performed using an Automatic Dicing Saw machine (DAD3350, Disco) with a 50 μm-thick diamond blade (226J-SE) at 3000 rpm. The dicing of the sapphire was performed in two steps due to the difficulty of cutting the sapphire. The first step used the dicing saw machine to produce grooves in the surface. The second step was to break the sapphire mechanically along the grooves using a blade (DORUCO)

dicing chuck.

To integrate the LED and the PV, a silver epoxy (EPO-TEK® E4110-PFC) with a high electrical conductivity and suitable viscosity was used. Silver epoxy bumps were placed on the n- and p- metal pads of the PV to prevent lateral spreading on pad interconnection. After bonding the LED and the PV, the stimulator was covered with a UV-curing epoxy (NOA68, Norland). The encapsulation epoxy is transparent to both NIR and blue light and biocompatible protecting the device and tissue following implant. A thin layer of the encapsulation epoxy was applied 5~7 times.

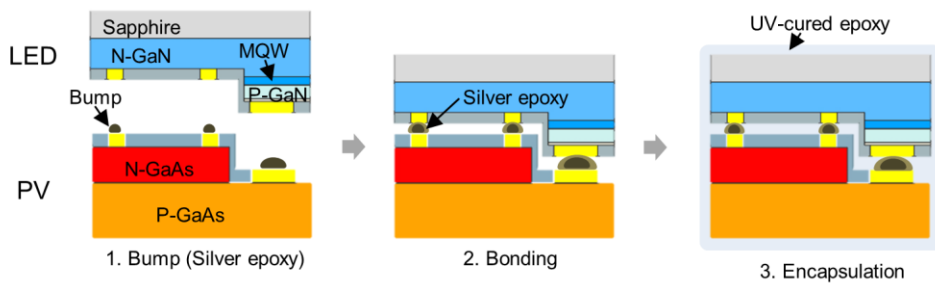

Figure 7. Schematic design of the bonding and encapsulation process of the LED to the PV cell.

2.5. Light source and measurement

To evaluate the characteristics of the PV, a TO-18 type 850 nm laser diode (LD) (from JDS Uniphase Corporation) is used to provide a NIR light source. The diode was protected from generating excessive heat using a temperature controlled mount and the injected current was driven by a laser diode controller (from THORLAB). Due to the large aspect ratio (~ 20) of the light irradiated from the LD, two cylindrical lenses having axes aligned perpendicular to each other were used. The focal lengths of the two lenses are 39 mm and 10 mm, respectively. After passing through the cylindrical lens, the NIR light beam was coupled to an optical fiber with a core diameter of 62.5 μm using an aspheric lens. The electroluminescence spectra of the LD and the LED were captured using an iHR-320 spectrometer (HORIBA). The intensity of the light output was measured by a Newport 1928 power meter. In order to investigate the electrical characteristics of the PV and the LED, a KEITHLEY 2425 source meter and a MS Tech probe station were used.

2.6. HEK cell culture and transfection for in-vitro electrophysiology experiment

HEK293 cells (ATCC) were cultured between 50% and 80% confluence in Dulbecco's Modified Eagle medium containing 10% FBS (Gibco), 1% penicillin/streptomycin (Invitrogen) in T25 tissue culturing flasks (SPL). Adherent cells were transfected within 12 to 24 hours with a complex of Lipofectaine2000 (Invitrogen) and pcDNA3.1-hChR2-EYFP (Addgene) plasmids in the culturing media. 2.7 μg of DNA plasmid was added to make transfection complexes. The expression of the ChR2-EYFP protein in HEK293 cells was verified by fluorescence microscopy (Nikon Ti-U). For electrophysiology recording of ChR2 with the stimulator, ChR2-EYFP expressed cells were plated at about 20-30% confluence on glass coverslips coated with poly-l-lysine (Sigma Aldrich). Whole-cell patch clamp experiments were conducted within 3 to 12 hours after being seeded on coverslips. HEK293 cells were bathed in extracellular solution containing at room temperature 150 mM NaCl, 4 mM KCl, 1 mM $MgCl_2$, 2 mM $CaCl_2$, 5 mM glucose, and 5 mM HEPES (pH7.4). A patch pipette was filled with internal solution containing 120 mM K-aspartate, 4 mM NaCl, 4 mM $MgCl_2$, 1 mM $CaCl_2$, 10 mM EGTA, 3 mM Na_2ATP, and 5 mM HEPES (pH 7.2). Whole-cell patch clamp recordings were performed using a Multiclamp 700B amplifier, Digidata 1440 digitizer, a PC operating

pClamp10 (Molecular Devices) with Lambda SC (Sutter) mechanical shutter. The simulator was placed under the cell mounted glass coverslip. A truncated optical fiber cable coupled to the 850 nm LD was mounted on the xyz stage holder of a micro-manipulator. The optical fiber was maneuvered and positioned near cells and the simulator. Blue light was emitted by the stimulator towards the cells when the 850 nm LD was turned on. The duration of blue light emission was controlled by modulating the 850 nm LD by the LAMBDA SC (Sutter) mechanical shutter.

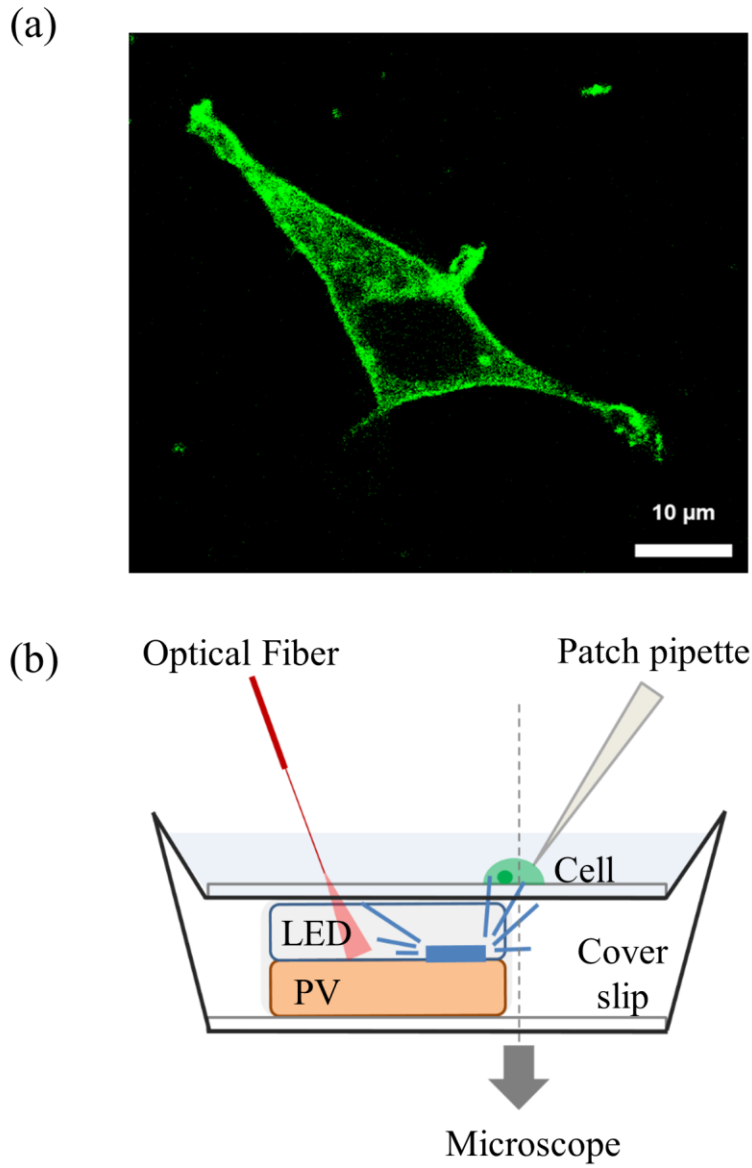

Figure 8. Electrophysiology of ChR2 with the Stimulator in a HEK293 cell. (a) Fluorescence image of a ChR2-EYFP expressed HEK293 cell, scale is 10 μm. (b) Schematic illustration of the optogenetic stimulation setup.

Chapter 3. Result and Discussion

3.1. Concavo-convex structure

The successfully fabricated the LED and PV have concavo and convex forms, respectively. Figure 9 (a) shows the concave form of the LED deep-etched ITO, p-type GaN, MQW, and a portion of n-type GaN with the exception of the 70×70 μm^2 emitting area. The PV has a convex form etched from the 6.28 μm-thick N-GaAs layer, with 95×95 μm^2 dimension as shown in Figure 9 (b)

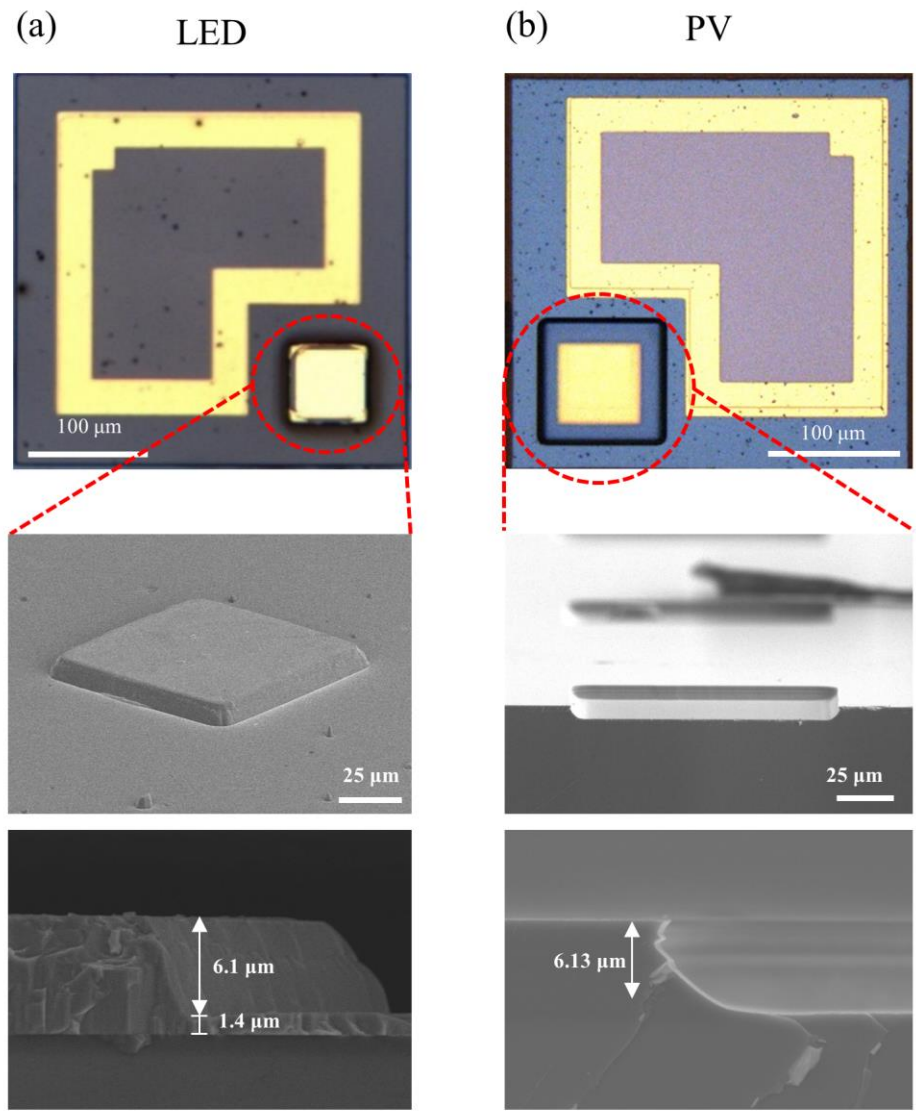

Figure 9. (a) Optical microscope image of top view and SEM image of the LED with 70×70 μm^2 light emitting area. (b) Optical microscope image and SEM image of top view of PV cell with 30000 μm^2 optical window for incident light after fabrication process.

3.2. **The characterization of LED and PV**

Figure 10 shows the characterization of the LED and PV after fabrication. The spectrum of the blue light emitted by the LED was measured and is shown in Figure 10 (a), the peak wavelength was found to be 449.2 nm, which is suitable for the stimulation of ChR2-expressing cells. The current-voltage-power characterization and performance of the LED, as displayed in Figure 10 (b), shows that the turn-on-voltage of the LED is 2.8 mV.

The relative efficiency was characterized by measuring the electrical output power of the PV cell under illumination by various wavelengths from 600 nm to 1000 nm using a monochromator. The PV cell is seen to have a high absorption rate for NIR light (820~850 nm) in comparison to other wavelengths of light as described by Figure 11 (a), The current-voltage performance of the PV cell under various input power conditions ranging from 0 mW to 6 mW, are shown in Figure 11 (b). At 6 mW, the short circuit current (Isc) is 768.7 μA and the open circuit voltage (Voc) is 3.145 V. The maximum energy conversion efficiency of the PV cell is around 34% and the output voltage provided by the PV cell is above 2.8 V, which is sufficient to turn the LED on.

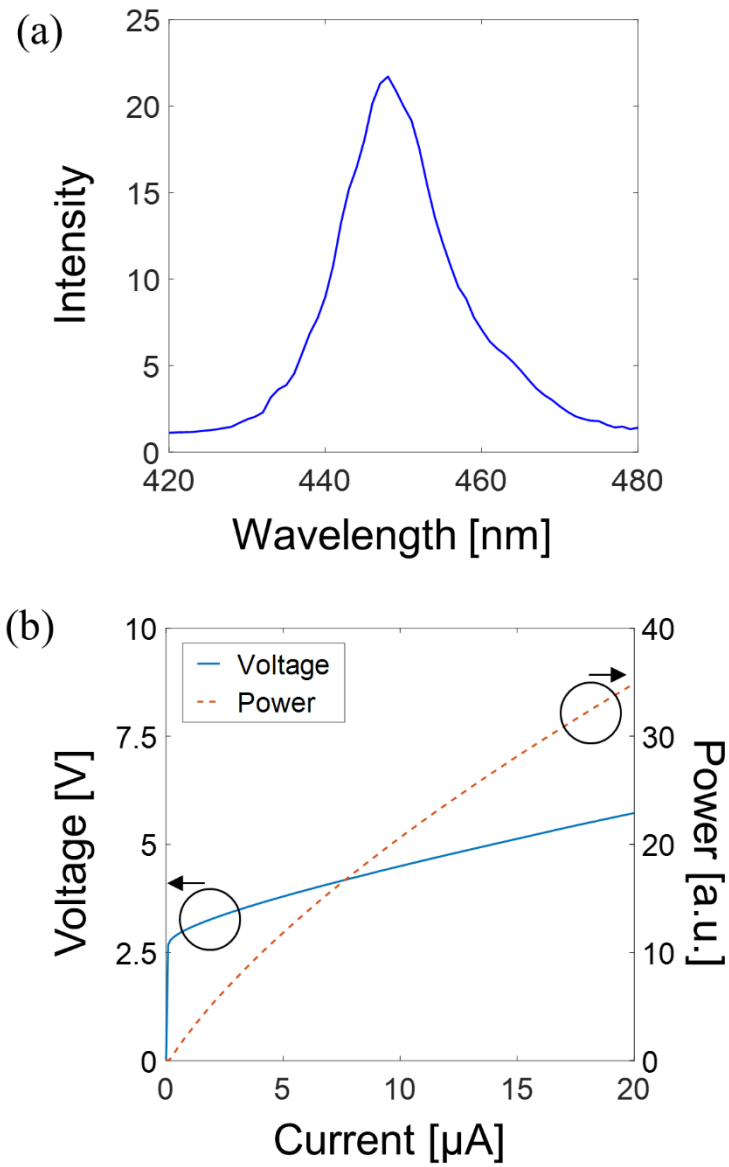

Figure 10. Characteristics of the LED. (a) Spectrum of light emitted from LED, the peak wavelength is 449.2 nm. (b) Current-voltage-power characteristics and performance of LED.

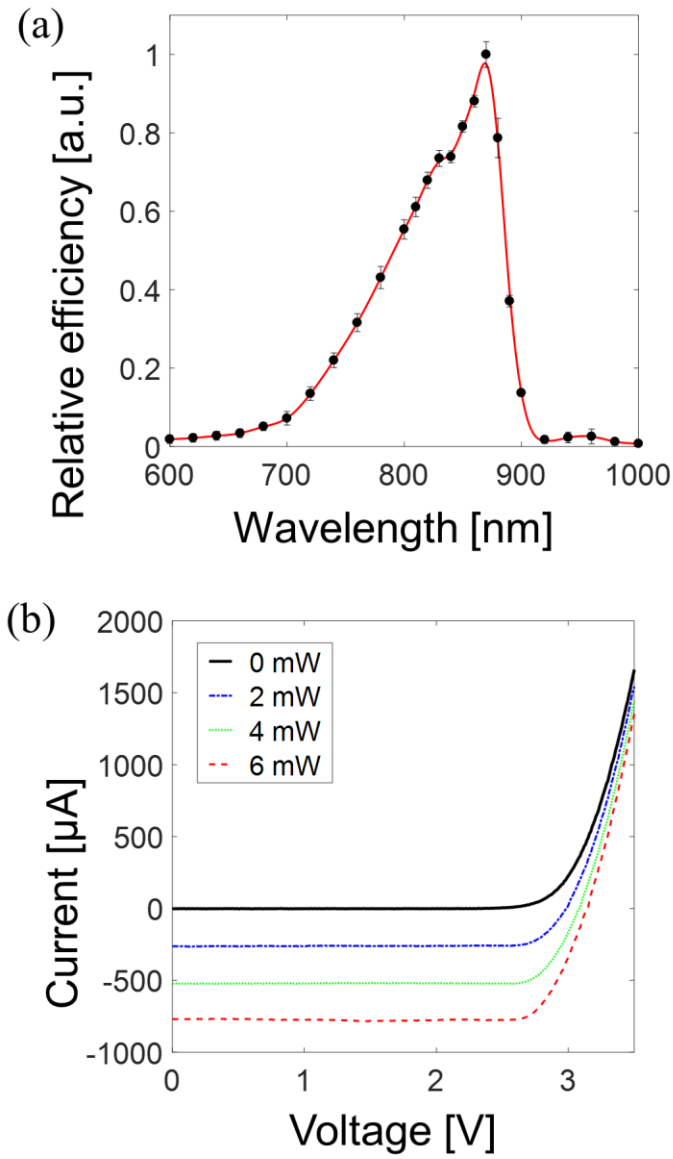

Figure 11. Characteristics of the PV cell. (a) Relative efficiency according to wavelength 600‑1000 nm; largest efficiency between 850~870 nm. (b) Voltage-Current characteristics and performance of PV cell; the PV cell has a fill factor of 0.84 and an efficiency of 34%.

3.3. **Structural result of integrated device**

The LED and PV each have dimensions of 400×400×200 μm^3, with their respective sizes controlled by the lapping and dicing processes. After bonding the LED to the PV using silver epoxy, the final dimensions of integrated stimulator were 400×400×400 μm^3. The stimulator coated with several UV-cured epoxy layers for encapsulation forms a 600 μm diameter sphere as shown in Figure 13.

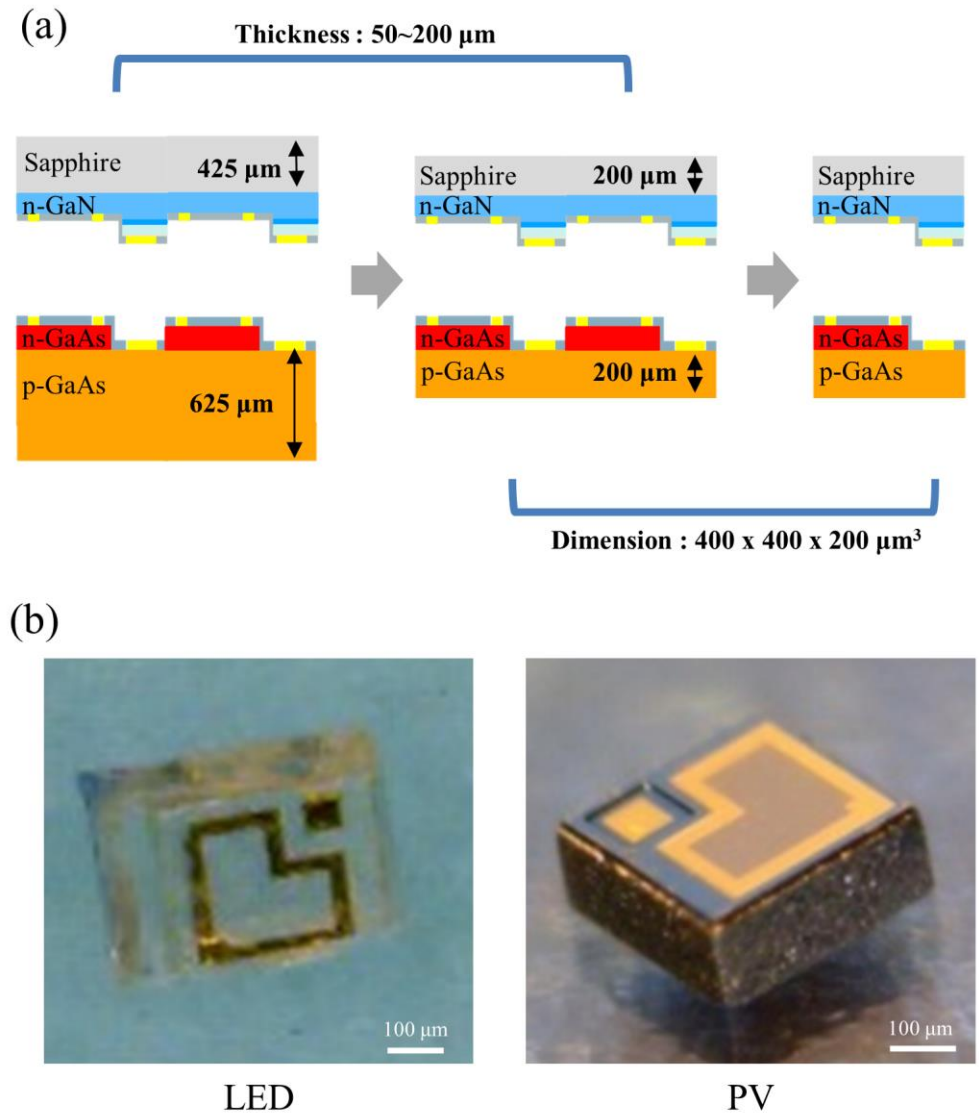

Figure 12. (a) Schematic design of the lapping and dicing process of the LED to the PV cell. (b) Optical image of isolated the LED and the PV cell after lapping and dicing process.

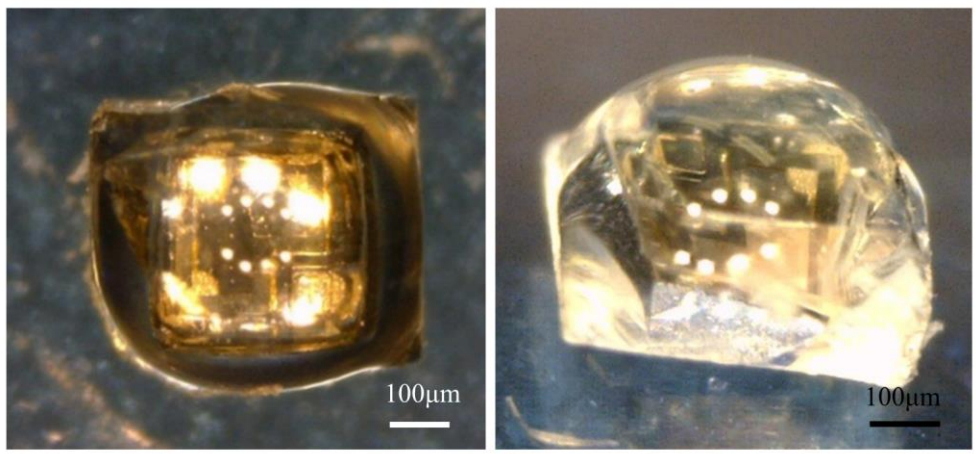

Figure 13. Optical image of the optoelectronic neural stimulator with dimension of a 600 μm diameter after encapsulation.

3.4. **Optoelectronic neural stimulator**

After bonding process, we tested the device to check that the LED and the PV were properly connected and the device was working properly in Figure 14. When 850 nm illuminated to the device, 450 nm light from device was emitted. It was confirmed that the 450nm light increases as the incident 850 nm light increase. It demonstrated that the PV absorbed 850 nm light and generated electrical energy, and the energy was transferred to the LED to emit blue light.

Figure 15 shows that the NIR light from the optical fiber was absorbed by the PV cell through the encapsulation layer and the LED and, that blue light was emitted from LED. The direction of the light emitted from the final device has been characterized. The result indicates the intensity of light emitted is greatest at the top and sides of the device. As shown in the horizontal plane, the intensity of light around the emitting area was 5 times higher. In the sagittal and coronal planes, the intensity of light at the top and around the sides was around 2 times higher than at the bottom.

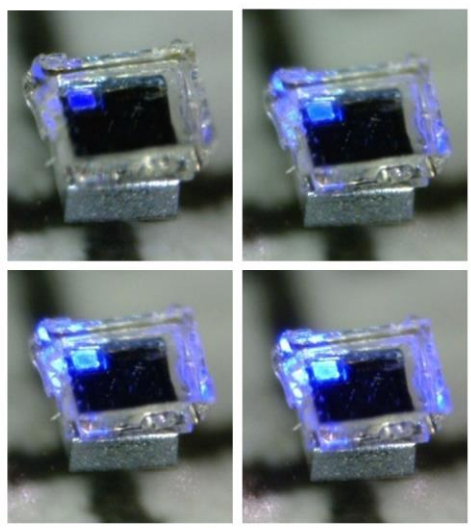

NIR light [mW]	Blue light [μW]
40	-
30	-
25	63
20	48
10	24
5	12

Figure 14. Optical image of integrated optoelectronic stimulator performance and power comparison of incident NIR light and emitting blue light.

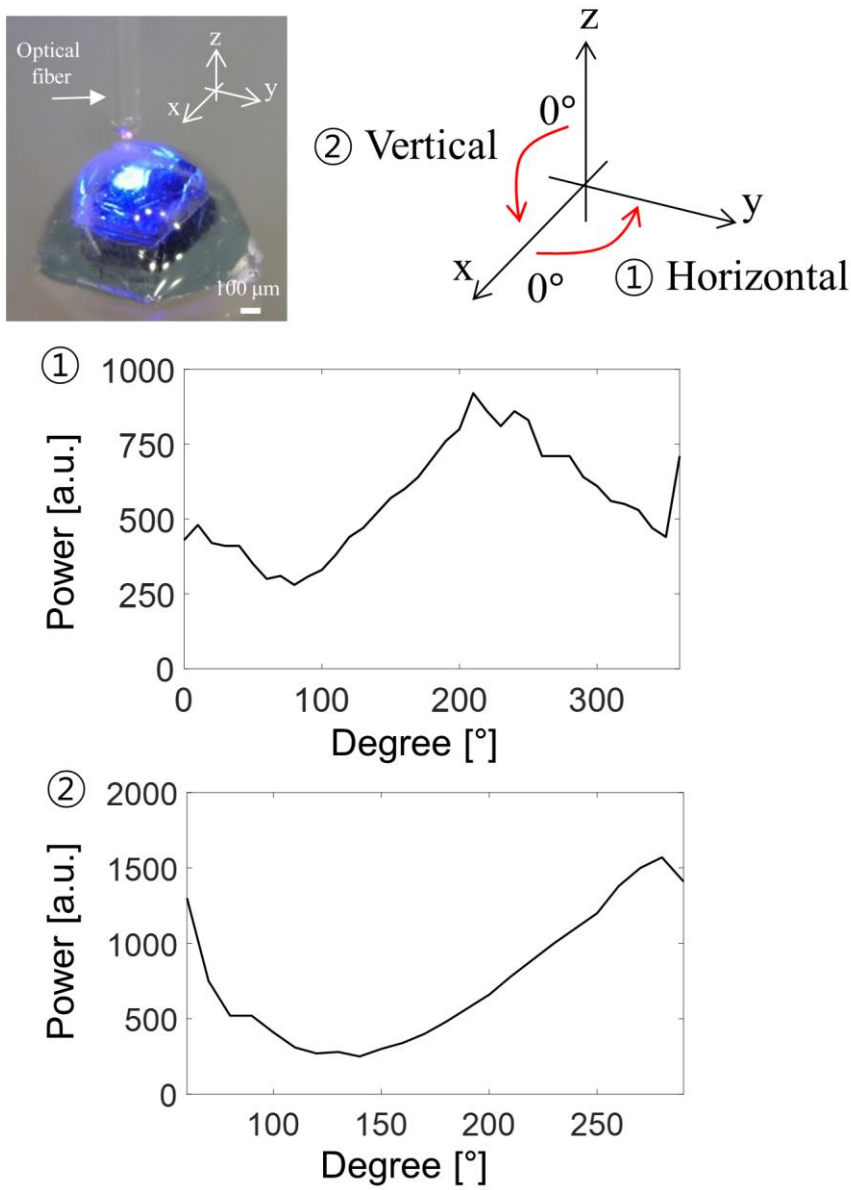

Figure 15. Optical image of stimulator coupled the optical fiber and xyz axis reference for the experiment of light emitting direction. And plot of intensity dependent on the direction of the emitting area of the LED in horizontal and vertical plane.

3.5. **In-vitro experiment**

In order to perform ChR2 electrophysiology experiments, the expression of ChR2-EYFP had to be verified. Under the confocal laser scanning microscope (ZEISS), the fluorescence of EYFP was detected. Especially, the blue light photosensitive membrane protein, ChR2, is well expressed in the membrane region and throughout the interior of the HEK293 cell. To test the ability of the stimulator to stimulate the cell, a whole-cell patch clamp experiment was conducted. During the 300 ms of 850 nm light illumination, the holding potential was raised from -100 (bottom) to +80 mV (top) in 20 mV steps as shown in Figure 16 (a). The photocurrents of the ChR2 were generated by the blue light from the stimulator at each holding potential. The intensity of the light was enough to modulate the ChR2, blue light sensitive cationic channel in HEK293 cells in vitro situation. When the holding potential was 100 mV, the induced maximum stationary photocurrent was measured at 420 pA. Since the ChR2 channel is a cationic channel, the negative holding potential setting of the whole-cell patch mode attracts more cations from the outside of the cell membrane into inside of the cell than a positive holding potential. Therefore, as the holding potential increases in 20 mV steps, the current-voltage characteristics in Figure 16 (b) show that the reversal potential was measured to be around 10 mV, which is typical for a ChR2 channel. The photocurrents induced by the stimulator would therefore be sufficient to evoke neuronal firing if it was implanted in the mammalian

brain.

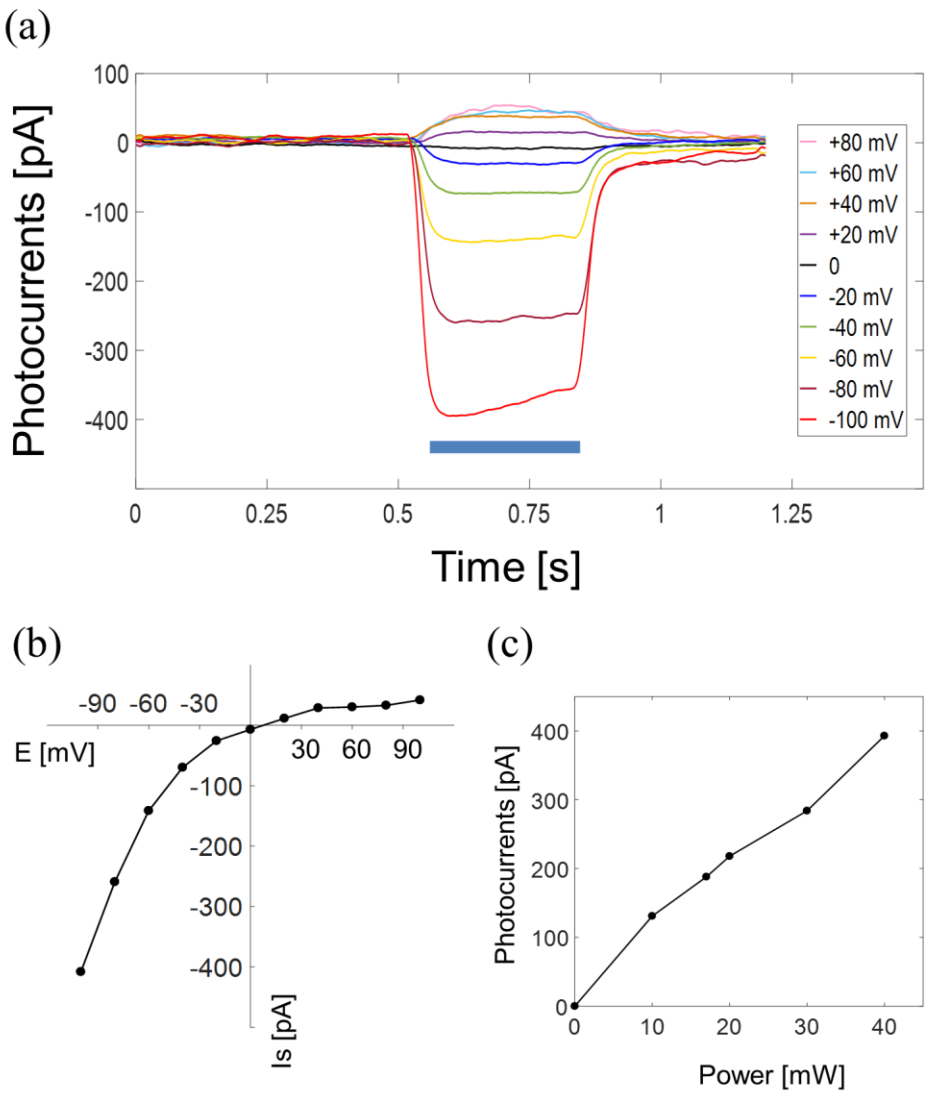

Figure 16. (a) ChR2 photocurrents at different holding potentials during 300 ms illumination. (b) Current-voltage characteristics of ChR2 during simulator illumination. (c) Photocurrents of ChR2 with 850 nm laser power at -100 mV holding potential.

Chapter 4. Conclusion

In this paper, an optoelectronic neural stimulator using a light absorbing PV cell and a light emitting LED has been developed. The PV cell absorbs 850~870 nm wavelengths of light, which is good for tissue penetration and the LED emits blue light (449.2 nm) to stimulate ChR2-expessing cells. The maximum power conversion efficiency of the PV cell is 34% at 6 mW of input power. In in-vitro experiments, the induced maximum stationary photocurrent was 420 pA at 100 mV of holding potential. This confirms that the device is able to stimulate target cells sufficiently. The developed optoelectronic stimulator in this paper can be fully utilized for long distance stimulation. The bonded stimulator has a concavo-convex structure, a dimension of 600 μm diameter sphere, and the micro-device structure means that tissue damage is minimized when it is implanted in the brain. It can help to provide a spatially precise analysis and functional understanding of relationships in neural networks. In the motor cortex, one pyramidal cell controls a muscle group associated a movement, it will help mapping neurons and muscle network. It can be used in the treatment of motor neuron diseases such as chorea and amyotrophic lateral sclerosis (ALS), and cerebral cortical disease such as Alzheimer's.

References

Abdo A, Sahin M, Freedman DS, Cevik E, Spuhler PS, Unlu MS (2011) Floating light-activated microelectrical stimulators tested in the rat spinal cord. Journal of neural engineering 8 (5):056012. doi:10.1088/1741-2560/8/5/056012

Anikeeva P (2013) Flexible optoelectronic devices for neural recording and stimulation. Flexible Electronics Session, NAE USFOE:1-13

AzimiHashemi N, Erbguth K, Vogt A, Riemensperger T, Rauch E, Woodmansee D, Nagpal J, Brauner M, Sheves M, Fiala A, Kattner L, Trauner D, Hegemann P, Gottschalk A, Liewald JF (2014) Synthetic retinal analogues modify the spectral and kinetic characteristics of microbial rhodopsin optogenetic tools. Nature communications 5:5810. doi:10.1038/ncomms6810

Boyden ES, Zhang F, Bamberg E, Nagel G, Deisseroth K (2005) Millisecond-timescale, genetically targeted optical control of neural activity. Nature neuroscience 8 (9):1263-1268. doi:10.1038/nn1525

Bruce RA, Piercy GR (1986) An improved AuGeNi ohmic contact to n type GaAs. Solid-State Electronics 30 (7):729-737

Cho HK, Lee JY, Lee B, Baek JH, Han WS (1999) Control of wet-etching thickness in the vertical cavity surface emitting laser structure by in situ laser reflectometry. Journal of Vacuum Science & Technology B: Microelectronics and Nanometer Structures 17 (6):2626. doi:10.1116/1.591036

Defelipe J (2011) The evolution of the brain, the human nature of cortical circuits, and intellectual creativity. Frontiers in neuroanatomy 5:29. doi:10.3389/fnana.2011.00029

Deisseroth K (2011) Optogenetics. Nature methods 8 (1):26-29. doi:10.1038/nmeth.f.324

Diester I, Kaufman MT, Mogri M, Pashaie R, Goo W, Yizhar O, Ramakrishnan C, Deisseroth K, Shenoy KV (2011) An optogenetic toolbox designed for primates. Nature neuroscience 14 (3):387-397. doi:10.1038/nn.2749

Eggert HR, Balazek V (1987) Optical properties of human brain tissue, menineges, and brain tumors in the spectral range of 200 to 900 nm. Neurosurgery 21 (459-464)

Han X, Qian X, Bernstein JG, Zhou HH, Franzesi GT, Stern P, Bronson RT, Graybiel AM, Desimone R, Boyden ES (2009) Millisecond-timescale optical control of neural dynamics in the nonhuman primate brain. Neuron 62 (2):191-198. doi:10.1016/j.neuron.2009.03.011

Huber D, Petreanu L, Ghitani N, Ranade S, Hromadka T, Mainen Z, Svoboda K (2008) Sparse optical microstimulation in barrel cortex drives learned behaviour in freely moving mice. Nature 451 (7174):61-64. doi:10.1038/nature06445

Kim TI, McCall JG, Jung YH, Huang X, Siuda ER, Li Y, Song J, Song YM, Pao HA, Kim RH, Lu C, Lee SD, Song IS, Shin G, Al-Hasani R, Kim S, Tan MP, Huang Y, Omenetto FG, Rogers JA, Bruchas MR (2013) Injectable, cellular-scale optoelectronics with applications for wireless optogenetics. Science 340 (6129):211-216. doi:10.1126/science.1232437

Kwon KY, Lee H-M, Ghovanloo M, Weber A, Li W (2014) A wireless slanted optrode array with integrated microLEDs for optogenetics. IEEE:813-816

Lee J, Ozden I, Song YK, Nurmikko AV (2015) Transparent intracortical microprobe array for simultaneous spatiotemporal optical stimulation and multichannel electrical recording. Nature methods 12 (12):1157-1162. doi:10.1038/nmeth.3620

Lu C, Froriep UP, Koppes RA, Canales A, Caggiano V, Selvidge J, Bizzi E, Anikeeva P (2014) Polymer fiber probes enable optical control of spinal cord and muscle function in-vivo. Advanced Functional Materials 24 (42):6594-6600. doi:10.1002/adfm.201401266

Lu Y, Kalkur TS, Paz de Araujo CA (1989) Rapid thermal alloyed ohmic contacts to p type GaAs. J Electrochem 136 (10)

Nagel G, Szellas T, Huhn W, Kateriya S, Adeishvili N, Berthold P, Ollig D, Hegemann P, Bamberg E (2003) Channelrhodopsin-2, a directly light-gated cation-selective membrane channel. Proceedings of the National Academy of Sciences of the United States of America 100 (24):13940-13945. doi:10.1073/pnas.1936192100

Packer AM, Roska B, Hausser M (2013) Targeting neurons and photons for optogenetics. Nature neuroscience 16 (7):805-815. doi:10.1038/nn.3427

Pisanello F, Sileo L, De Vittorio M (2016) Micro- and nanotechnologies for optical neural interfaces. Frontiers in neuroscience 10:70. doi:10.3389/fnins.2016.00070

Schneider F, Grimm C, Hegemann P (2015) Biophysics of channelrhodopsin. Annual review of biophysics 44:167-186. doi:10.1146/annurev-biophys-060414-034014

Shiraishi Y, Taeda T (1998) Low resistance thermally stable ohmic contact to n GaAs for low cost high density interconnections. GaAs Mantech:271-220

Son Y, Lee HJ, Kim D, Kim YK, Yoon E-S, Kang JY, Choi N, Kim TG, Cho I-J (2014) MEMS neural probe array for multiple-site optical stimulation with low-loss optical waveguide by using thick glass cladding layer. IEEE:853-856

Song YK, Stein J, Patterson WR, Bull CW, Davitt KM, Serruya MD, Zhang J, Nurmikko AV, Donoghue JP (2007) A microscale photovoltaic neurostimulator for fiber optic delivery of functional electrical stimulation. Journal of neural engineering 4 (3):213-218. doi:10.1088/1741-2560/4/3/006

Wang J, Wagner F, Borton DA, Zhang J, Ozden I, Burwell RD, Nurmikko AV, van Wagenen R, Diester I, Deisseroth K (2012) Integrated device for combined optical neuromodulation and electrical recording for chronic in vivo applications. Journal of neural engineering 9 (1):016001. doi:10.1088/1741-2560/9/1/016001

Warden MR, Cardin JA, Deisseroth K (2014) Optical neural interfaces. Annual review of biomedical engineering 16:103-129. doi:10.1146/annurev-bioeng-071813-104733

Yamaguchi M (1999) Physics and technologies of superhigh-efficiency tandem solar cells_semiconductors. Semiconductors 33 (9):961-964

Zhang J, Laiwalla F, Kim JA, Urabe H, Van Wagenen R, Song YK, Connors BW, Zhang F, Deisseroth K, Nurmikko AV (2009) Integrated device for optical stimulation and spatiotemporal electrical recording of neural activity in

light-sensitized brain tissue. Journal of neural engineering 6 (5):055007. doi:10.1088/1741-2560/6/5/055007

요약 (국문초록)

생체 광유전학 연구를 위한 발광다이오드와 광전지가 집적된 광전자 신경 자극기의 개발

빛을 이용한 광유전학방법은 전기적 자극을 이용한 방법과는 달리 목표하는 세포만을 자극할 수 있는 새로운 자극 패러다임을 제공했다. 이 논문에서는 광전지 셀(PV)과 발광다이오드(LED)를 이용한 생체 광유전학 연구를 위한 무선 임플란트 광전자 신경 자극기를 개발에 대한 얘기를 한다. 자극기에서 세포를 자극하기 위해 u-LED를 이용하였으며 이 LED를 켜기 위해 PV를 함께 결합시켰다. PV는 GaAS기반으로 티슈투과율이 높은 근적외선 빛을 흡수하도록 디자인되어 있으며, 빛의 흡수율을 높이기 위해 최적화된 높이를 가진 3개의 층으로 구성된 텐덤 구조로 제작되었다. 이 자극기는 광전지과 발광다이오드를 집적 시켜 뇌 안에 전체 임플란트 할 수 있는 400um 변을 가진 마이크로 사이즈의 정육면체 형태로 디자인되었다. 이는 조직 손상을 줄일 수 있을 뿐만 아니라 무선으로 연결되어 실험 체의 활동범위를 제한하지 않는 다는

장점을 가지고 있다. 마이크로공정법의 Deep etching 방법을 이용하여 PV와 LED가 P-P junction를 구성할 수 있도록 요철모양으로 본딩 하였다. 공정 이후 실험을 통해 PV는 34%의 고효율을 내며 LED를 켜기 위해 충분한 에너지를 낼 수 있다는 것을 확인 하였으며 HEK cell와 패치 클램프를 이용하여 자극기 푸른빛이 세포를 자극 할 수 있다는 결과를 보여줬다.

주요어 : 광유전학, 광전자, 신경 자극, 광기전성 셀, 발광다이오드, 생체 이식

학 번 : 2014-24885